Available online at www.sciencedirect.com
SCIENCE DIRECT
Vision Research 46 (2006) 2546–2553
Vision Research
www.elsevier.com/locate/visres

Optical aberrations in the mouse eye

Elena García de la Cera [a], Guadalupe Rodríguez [b], Lourdes Llorente [a], Frank Schaeffel [c], Susana Marcos [a,*]

[a] Instituto de Óptica "Daza de Valdés," Consejo Superior de Investigaciones Científicas, Madrid, Spain
[b] Instituto Universitario de Oftalmobiología Aplicada, Universidad de Valladolid, Valladolid, Spain
[c] Section of Neurobiology of the Eye, University Eye Hospital, Tübingen, Germany

Received 1 October 2005; received in revised form 10 January 2006

Abstract

Purpose: The mouse eye is a widely used model for retinal disease and has potential to become a model for myopia. Studies of retinal disease will benefit from imaging the fundus in vivo. Experimental models of myopia often rely on manipulation of the visual experience. In both cases, knowledge of the optical quality of the eye, and in particular, the retinal image quality degradation imposed by the ocular aberrations is essential. In this study, we measured the ocular aberrations in the wild type mouse.

Methods: Twelve eyes from six four-week old black C57BL/6 wild type mice were studied. Measurements were done on awake animals, one being also measured under anesthesia for comparative purposes. Ocular aberrations were measured using a custom-built Hartmann–Shack system (using 680-nm illumination). Wave aberrations are reported up to fourth order Zernike polynomials. Spherical equivalent and astigmatism were obtained from the 2nd order Zernike terms. Modulation Transfer Functions (MTF) were estimated for the best focus, and through-focus, to estimate depth-of-focus. All reported data were for 1.5-mm pupils.

Results: Hartmann–Shack refractions were consistently hyperopic (10.12 ± 1.41 D, mean and standard deviation) and astigmatism was present in many of the eyes (3.64 ± 3.70 D, on average). Spherical aberration was positive in all eyes (0.15 ± 0.07 μm) and coma terms RMS were significantly high compared to other Zernike terms (0.10 ± 0.03 μm). MTFs estimated from wave aberrations show a modulation of 0.4 at 2 c/deg, for best focus (and 0.15 without cancelling the measured defocus). For that spatial frequency, depth-of-focus estimated from through-focus modulation data using the Rayleigh criterion was 6 D. Aberrations in the eye of one anesthetized mouse were higher than in the same eye of the awake animal.

Conclusions: Hyperopic refractions in the mouse eye are consistent with previous retinoscopic data. The optics of the mouse eye is far from being diffraction-limited at 1.5-mm pupil, with significant amounts of spherical aberration and coma. However, estimates of MTFs from wave aberrations are higher than previously reported using a double-pass technique, resulting in smaller depth-of-field predictions. Despite the large degradation imposed by the aberrations these are lower than the amount of aberrations typically corrected by available correction techniques (i.e., adaptive optics). On the other hand, aberrations do not seem to be the limiting factor in the mouse spatial resolution. While the mouse optics are much more degraded than in other experimental models of myopia, its tolerance to large amounts of defocus does not seem to be determined entirely by the ocular aberrations.
© 2006 Elsevier Ltd. All rights reserved.

Keywords: Mouse eye; Optical quality; Ocular aberrations; Myopia model; Refractive state; Depth of focus

1. Introduction

The mouse is the most widely used animal model for human diseases, including inherited vision disorders. Its genome has been almost completely sequenced and there are many transgenic models available. For example, mouse models of retinal degeneration have been investigated for many years in the hope of understanding the causes of photoreceptor cell death (Chang et al., 2002). There are also knockout mouse models for cataracts (Hegde, Henein, & Varma, 2003), glaucoma (Lindsey & Weinreb,

* Corresponding author.
E-mail address: susana@io.cfmac.csic.es (S. Marcos).

0042-6989/$ - see front matter © 2006 Elsevier Ltd. All rights reserved.
doi:10.1016/j.visres.2006.01.011

2005), and diabetic retinopathy (Kern & Engerman, 1996). Also, there are recent efforts to develop a mouse myopia model by visual deprivation (Beuerman, Barathi, Weon, & Tan, 2003; Schaeffel, Burkhardt, Howland, & Williams, 2004).

Electrophysiological (Porciatti, Pizzorusso, & Maffei, 1999) and behavioral studies (Gianfranceschi, Fiorentini, & Maffei, 1999; Prusky, Alam, Beekman, & Douglas, 2004; Schmucker & Schaeffel, 2006) indicate that the visual spatial resolution in the wild type mouse is poor, and the debate is open whether the optics of the eye match the coarse resolution of the neural mosaic (Artal, Herreros de Tejada, Muñoz-Tedo, & Green, 1998). Knowledge of the retinal image quality in the mouse is important for various reasons. First, it will help to clarify the limits of spatial vision in the mouse. Second, the measurement of the aberrations of the mouse eye and their potential correction by means of adaptive optics (Roorda & Willians, 2001) or phase-plates (Burns, Marcos, Elsnser, & Bará, 2002) will open the possibility of applying new in vivo retinal imaging methods. In vivo observations of critical retinal features in mice with retinal degenerations, glaucoma or diabetic retinopathy will allow a better understanding of the pathogenesis, and longitudinal measurements of associated changes and effects of drug therapies, not possible in the cross-sectional data provided by histology (Burns et al., 2004; Ritter et al., 2005; Seeliger et al., 2005). However, the application of the current correction technology to mice eyes, and the resolution of the fundus images will be limited by the actual amounts of aberrations present in these eyes. Finally, most frequent myopia models rely on the ability of the ocular growth mechanisms to respond to visual experience. However, optical aberrations determine to a great extent the depth-of-focus of the eye (Marcos, Barbero, & Jimenez-Alfaro, 2005; Marcos, Moreno, & Navarro, 1999) and the effects of defocus on retinal image quality will be drastically different whether the eye is diffraction-limited or highly aberrated.

Despite the need for a clearer understanding on the degradation imposed by the optics of the mouse on the retinal image, there are very limited studies that have attempted to assess it, and none, to our knowledge has measured the optical aberrations in the mouse. The very few studies available suggest that the optics of the rodent eye are highly degraded (Artal et al., 1998). Hughes and Wassle (1979) reported drastic drop in the contrast of grating targets projected on rat retinas and observed by indirect retinoscopy. Schmucker and Schaeffel (2004b) reported photoretinoscopic reflexes consistent with high amounts of aberrations.

A recent report (Irving, Kisilak, Clements, & Campbell, 2005) shows very distorted Hartmann–Shack images and consequently high amounts of aberrations in the awake rat eye. To our knowledge, the only published study on the objective retinal image quality of the rodent eye (six 3-month Long Evans rats and three C57BL/6J mice of the same age) was performed using a double-pass system (Artal et al., 1998). Animals were fully anesthetized. By recording through-focus double-pass aerial images of a point source they found very little optical quality change (less than 10%) across 24 D, with a slight tendency of optical quality to increase with hyperopic corrections (although they failed at finding a "best focus"). Large depth-of-focus in the rat eye (±10 D) had been predicted by Green et al. (Green, Powers, & Banks, 1980). Remtulla and Hallett (1985) predicted a depth-of-focus of ±56 D in adult mice based on eye size and photoreceptor diameters, or ±11 D once differences between behavioral and ganglion cell acuity were taken into account. Other studies report ±10 D from whole-body optomotor responses (Schmucker & Schaeffel, 2006). Hyperopic defocus has also been reported using streak retinoscopy and IR photoretinoscopy in mice, with refractive states ranging from +15.0 D in adult Balb/CJ mice (Beuerman et al., 2003), +13.5 D in 30-day-old C57BL/6J mice (Tejedor & de la Villa, 2003), or +7.0 D in 70-day-old mice (Schmucker & Schaeffel, 2004b). However, these hyperopic refractions do not match those estimated by visual evoked potentials (Mutti, VerHoeve, Zadnik, & Murphy, 1997), which are closer to emmetropia. This difference has been attributed to relatively large distance between the photoreceptor plane layer and the retinal layer where the retinoscopic reflection potentially takes place.

The only experimental modulation transfer functions (MTFs) available in the rodent eye (mostly rat's and one example for one mouse) were obtained on anesthetized animals (Artal et al., 1998). This study reports modulations of less than 0.1 for the mouse and 1 for the rat at 1 c/deg, for 1-mm pupils. In the double-pass method, MTFs are estimated from the intensity distributions of the aerial images of a point source reflected by the retina, and therefore highly dependent on retinal scattering. It is questionable however whether this veiling pedestal affecting the double-pass aerial image truly represents the actual point spread function of the ocular optics.

Provided that the ocular media are clear, and intraocular scattering is not a major source of retinal image degradation, MTFs obtained from wave aberrations will account for the actual contrast losses caused by the ocular optics in the mouse, unaffected by retinal scattering. In addition, the measurement of individual aberrations in the mouse eye will allow us to better understand the sources of optical degradation. A previous study (Artal et al., 1998) attempted to predict aberrations in the rat eye using a simple eye model and biometric data provided by Hughes (1979). Those simulations found significant amounts of spherical aberration due to the highly curved surfaces of small eyes. However, the predicted MTFs were higher than the experimental MTFs, that led the authors to conclude that other unknown high order aberrations were also present. Currently, new biometric data in the mouse are available using new technology (Lin et al., 2004; Schmucker & Schaeffel, 2004a). For example, for typical 4-week-old mouse, reported ocular dimensions are: axial length = 3.02 mm, anterior chamber

depth = 0.20 mm, lens thickness = 1.77 mm, and corneal radius of curvature 1.41 mm (Lin et al., 2004; Schmucker & Schaeffel, 2004a). Predictions based on eye models could be revisited in the light of those biometric data and the ocular aberrations reported here. Finally, measurements of the wave aberrations will allow us to obtain the refractive state of mice, from the defocus term in the polynomial expansion describing the wave aberration function, and also to estimate the depth-of-focus, by computing through-focus optical quality as the defocus term is computationally changed in the wave aberration function.

2. Methods

2.1. Subjects

Black C57BL/6 wild type mice were obtained from Charles River, Barcelona, Spain, and kept in the animal facilities of the Instituto de Oftalmobiología Aplicada, Universidad de Valladolid, Spain, housed in standard mouse cages under 12 h light/dark cycle. All experimental protocols were approved by the Institutional Review Boards, and met the ARVO resolution for care and use of laboratory animals. Six four-week old females were used in this study.

2.2. Hartmann–Shack aberrometer

Ocular aberrations were measured with a Hartmann–Shack aberrometer built at the Instituto de Óptica (Consejo Superior de Investigaciones Científicas), Madrid, Spain. This system was used before to measure ocular aberrations in normal and myopic chick eyes, and has been described in detail elsewhere (García de la Cera, Rodriguez, & Marcos, 2006). A schematic diagram of the device can be found in Fig. 1 of that publication.

In brief, the illumination source is a 676-nm superluminescent diode, and the Hartmann–Shack image is collected by a high-resolution CCD camera. Defocus of the exit beam can be corrected (from −7 to +9 D) by a Badal system, although for this study this correcting device was not used and defocus was directly obtained from the data. The microlens array placed on a pupil conjugate plane consists of 65 × 65 square microlenses with 24-mm focal length and 400-μm aperture. The pupil, illuminated by an LED ring, is continuously monitored by a CMOS camera. The HS image capture, pupil monitoring, and the electronic shutter are controlled by a computer using a custom-developed program written in Visual Basic (Microsoft Corporation, Redmond, Washington). The particularly low quality of the Hartmann–Shack spots from mouse eyes prevented to use the more standard processing algorithms developed previously (García de la Cera et al., 2006). Therefore, new routines for HS spot detection and centroiding algorithms specifically developed for the present study were written in Matlab (Mathworks, Natick MA). Shifts of the centroids were estimated with respect to the corresponding Hartmann–Shack spots produced by an artificial eye that acted as a reference. The artificial eye consisted of a diffraction-limited lens (achromatic doublet, 50-mm focal

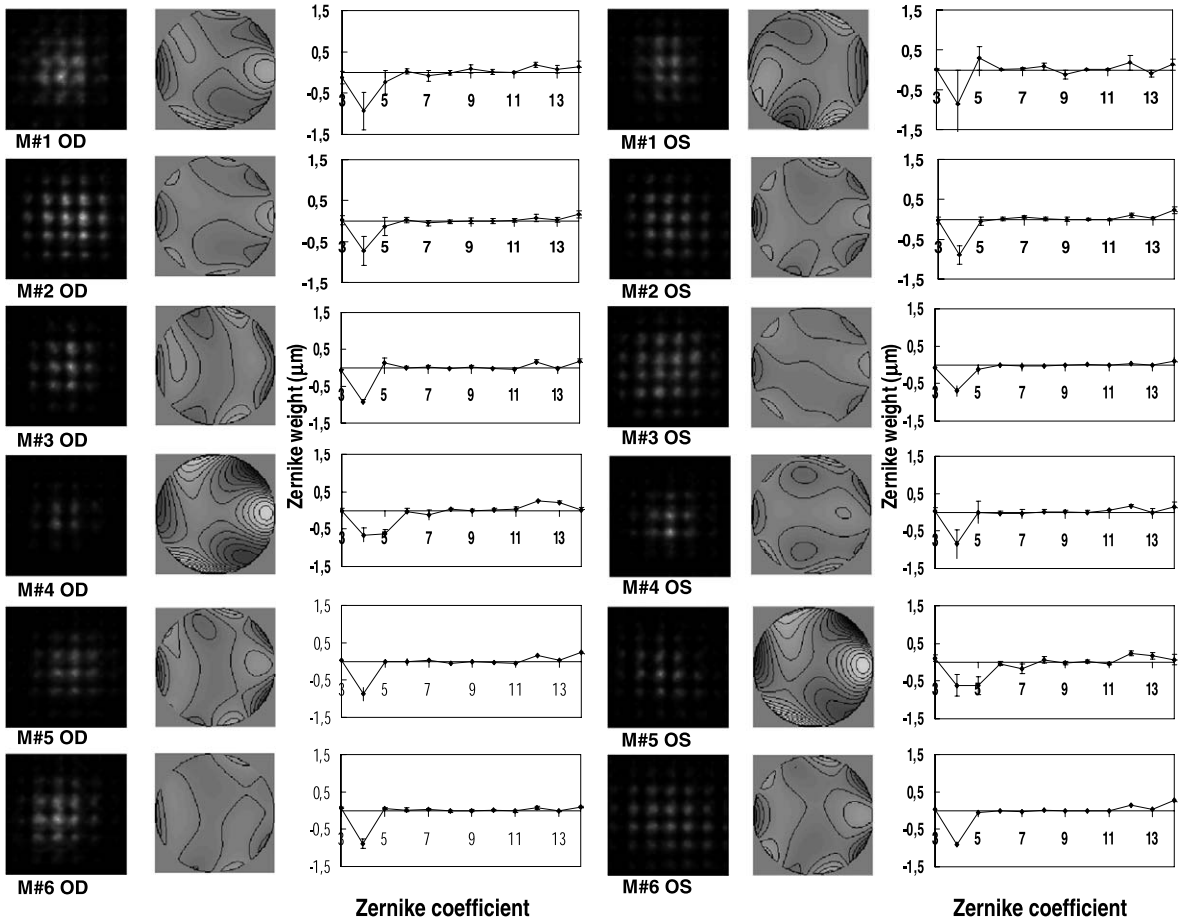

Fig. 1. Examples of Hartmann–Shack images on awake mouse eyes, and corresponding wave aberration maps and mean Zernike coefficients. OD and OS stand for the right and left eye, respectively. Images were captured with pupil sizes ranging from 1.63 to 2.17 mm. Wave aberration maps are for third and higher order aberrations, and contour lines are plotted in 0.1 μm steps. Zernike coefficients are ordered following the OSA convention (single indexing scheme), and the error bars stand for standard deviations. Aberration data are for 1.5-mm pupil diameters and 678 nm.

length, 12.5 mm diameter, Newport Corporation) with a diffuser at its focal plane. The centroid of each retinal spot was located by fitting the intensity profiles to a gaussian function. Zernike coefficients were obtained by modal fitting of the lateral deviations to the derivatives of the Zernike polynomial expansion.

The accuracy of the system was tested on spherical and cylindrical trial lenses, as well as lenses with known amounts of high order aberrations. In particular, control experiments were performed in the presence of large amounts of hyperopic defocus, which mimicked that typically found in the mouse eye. Comparisons between a Hartmann–Shack system and a validated Laser Ray Tracing system in the laboratory have been previously published (Llorente, Diaz-Santana, Lara-Saucedo, & Marcos, 2003; Marcos, Díaz-Santana, Llorente, & Dainty, 2002; Moreno-Barriuso, Marcos, Navarro, & Burns, 2001).

2.3. Experimental protocols

Mice were measured in the Hartmann–Shack system under awake and normal viewing conditions, i.e., without anesthesia nor with cyclopegia. The animals were restrained by holding their tails while they were sitting on an elevated platform mounted in front of the system, which allowed centration and focusing of the animal's pupil. The pupil image channel provided continuous pupil monitoring and let us to control Purkinje images from the IR ring during measurements. We made sure that the Purkinje images remained within the pupil, as we used this as an indication that fixation was not excessively eccentric. Additional centration could be achieved by moving the x–y stage that translates the entire Hartmann–Shack system. After some adaptation to the task, the mice became cooperative and did not move during the measurement, allowing us to capture several (5–10) images per eye. The same procedure was repeated for left and right eyes.

For comparative purposes, mouse labelled as # 2 was also measured under anesthesia. The animal was anesthetized with a subcutaneous injection of a mixture of 1.2 ml of 10% ketamine hydrochloride and 0.8 ml 2% xylacine hydrochloride, dissolved in 8.0 ml sterile saline. In those measurements, eyelids were held open and the cornea was moistened with eye drops (Viscofresh 0.5%, Allergan).

2.4. Data analysis

Typical Hartmann–Shack images contained up to 15 spots. In general, images from the same eye were very similar, suggesting a good fixation by the animal. Data were processed for the maximum pupil diameter (ranging from 1.63 to 2.17 mm) and then re-scaled for the minimum pupil size available (1.5 mm) to allow a direct comparison across all eyes. Reported data for each eye are averages of at least five individual measurements. The optical quality of the eye was assessed in terms of individual Zernike coefficients and the root-mean-square wavefront error (RMS) of the different terms or orders. Modulation transfer functions (MTF) and point spread functions (PSFs) were also obtained from the wave aberrations. The volume under the MTF and the modulation at 2 c/deg were also used as an optical quality metric. Through-focus estimates of these metrics were used to compute depth-of-focus.

3. Results

3.1. Hartmann–Shack images and wave aberrations

Fig. 1 shows the Hartmann–Shack raw data, clearly more degraded than those typically found in human eyes (Liang & Williams, 1997), chicks (García de la Cera et al., 2006), rhesus monkeys (Vilupuru, Roorda, & Glasser, 2004) or cats (Huxlin, Yoon, Nagy, Porter, & Williams, 2004). HS images were obtained for pupil diameters ranging from 1.63 to 2.17 mm. The corresponding wave aberrations for third and higher order (for 1.5 mm pupils) show prevalence of positive spherical aberration (coefficient #12 in the plot) in most of the animals, as well as significant amounts of other high order aberrations, even for these small pupil sizes. Zernike coefficients following the Optical Society of America notation (Thibos, Applegate, Schwiegerling, Webb, & Members, 2000) are also shown in all eyes (averaged across measurements in each eye, and the error bars corresponding to the standard deviation).

3.2. Refractive state

Zernike coefficient Z_2^0 (#4 in single indexing scheme), corresponding to the defocus term (with negative sign, consistent with hyperopic defocus), is the largest aberration in all eyes, as shown in Fig. 1. Fig. 2 shows the average spherical equivalent found for each eye, computed from the defocus term of the Zernike polynomial expansion, and for a wavelength of 678 nm. The spherical equivalent is consistently hyperopic in all eyes, $+10.12 \pm 1.41$ D (average $\pm$ standard deviation). Intersubject variability is of the order of the average interocular differences (1.97 D) and smaller than the average measurement variability (2.61 D). Astigmatism was computed from Zernike terms Z_2^1 and Z_2^{-1} (#3 and 5) and found to be on average 3.64 ± 3.70 D. Taking the measured astigmatism into account, pure spherical error resulted in $+8.30 \pm 3.00$ D. We did not find a preference for the horizontal or vertical meridian to be the least hyperopic. The astigmatism axis tended to be mirror symmetric across left and right eyes. Astigmatism axis values are clustered around 37 ± 4 deg and -37 ± 9 deg (or 127 ± 9 deg in the positive cylinder convention) in all eyes except one (mouse#4, left eye).

3.3. High order aberrations

Fig. 3 shows root mean square wavefront errors (RMS) for different terms and all eyes, for 1.5-mm pupils. Average third and higher order aberrations RMS is 0.32 ± 0.08 μm. Spherical aberration accounts for a significant proportion of the high order aberrations (0.15 ± 0.06 μm), equivalent to a blur of 1.85 D. However, third order aberrations alone (RMS $= 0.13 \pm 0.04$ μm) represent also a major source of

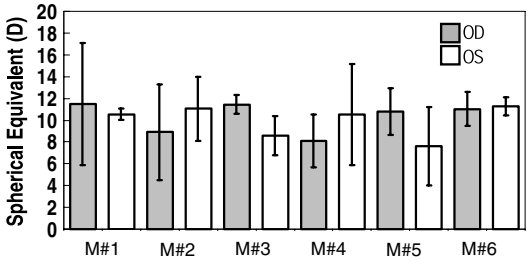

Fig. 2. Spherical error for all mice obtained from the defocus Zernike term. Gray bars correspond to right eyes and white bars to left eyes. Error bars stand for standard deviations across measurements.

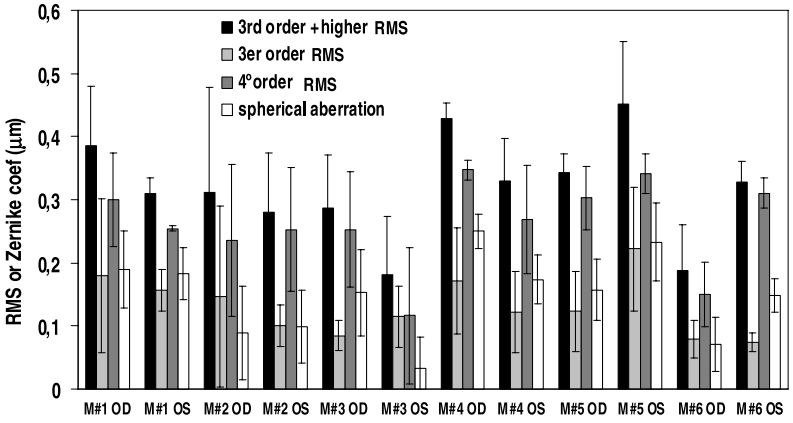

Fig. 3. Mean third and higher order RMS (black bars), third order RMS (light gray bars), fourth order RMS (dark gray bars), and spherical aberration Zernike coefficient (white bars). Error bars represent intersubject variability and stand for standard deviations across eyes. Data are for 1.5-mm pupil diameters.

degradation, particularly coma (RMS = 0.10 ± 0.03 μm), and other non-spherical fourth order terms are also relatively important. High order aberration intersubject variability is low and comparable with variability of repeated measurements on the same eye (0.07 μm, on average).

3.4. Modulation transfer functions

Fig. 4 shows average radial-profile modulation transfer functions (MTFs) across all eyes obtained from wave aberrations, for 1.5 mm pupils and for the illumination wavelength (678 nm). Average best focus MTF (i.e., correcting for hyperopic defocus) is shown in black solid line, and average non-corrected MTF (i.e., with all low and higher order aberrations) is shown in black dotted lines. For proper comparison of MTFs, it should be noted that the mouse eye has a particularly low numerical aperture (NA = 0.5). MTFs for 1.5 mm pupils in another small eye (chick eye, NA = 2.6) measured with the same Hartmann–Shack apparatus and the average human eye MTFs for 6.5-mm pupil diameter (NA = 3.4) are also shown for comparison, along with the diffraction-limited MTF for 1.5 and 6.5 mm pupils. As a reference, the diffraction-limited MTF with the same amount of defocus (10 D) as found in the mouse eye has also been included, for 1.5 mm. In the mouse, while defocus imposes additional optical degradation, major losses in contrast are produced by high order aberrations alone (see black solid line). Also, interactions of high order aberrations and defocus produce significant differences beyond 1 c/deg between the real mouse eye with defocus and the diffraction-limited eye with the same amount of defocus (compare black and gray dotted lines).

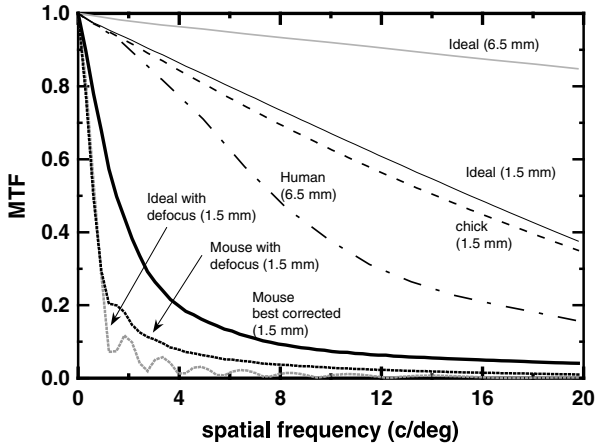

Fig. 4. Mean MTFs (radial profile) averaged across all mouse eyes for best focus (black solid line), and uncorrected defocus (black dotted line) for 1.5 mm pupil diameter. For comparison average MTF for four-week old chicks ($n = 5$) for 1.5 mm-pupils (dashed line) from wave aberrations measured with the same Hartmann–Shack system (García de la Cera et al., 2006), MTF for young human eyes for 6.5-mm pupils measured with a Laser Ray Tracing system (dotted-dashed line) (Barbero et al., 2003). Theoretical MTFs of a diffraction-limited eye for 1.5-mm pupil (gray thin line), of a diffraction-limited eye for 6.5-mm pupil (black thin line), and a diffraction-limited eye with +10 D of defocus (gray dotted line) are also represented. MTFs were computed for 680 nm.

3.5. Depth-of-focus

Through-focus image quality estimated by computationally changing the defocus term (at 1 D steps) in the wave aberration, for 1.5-mm pupils, is represented in Fig. 5. Modulation transfer for 2 c/deg, same spatial frequency used by Artal et al. (1998) for the rat eye, was used as an image quality metric. The curves in Fig. 5 are referred to zero defocus, i.e., compensating the spherical error given by the defocus term in each eye. However, in most eyes, the highest optical quality does not correspond to that correction, as typically found in the presence of high order aberrations (Guirao & Williams, 2003). We found best-optical quality to be shifted on average 0.42 D toward less hyperopic values.

Depth-of-focus was estimated using the Rayleigh criterion, i.e., as the defocus range for which optical quality was at least 80% of the value at best focus (Marcos et al., 1999) and ranges from 4.5 to 7.9 D. The volume under the MTF

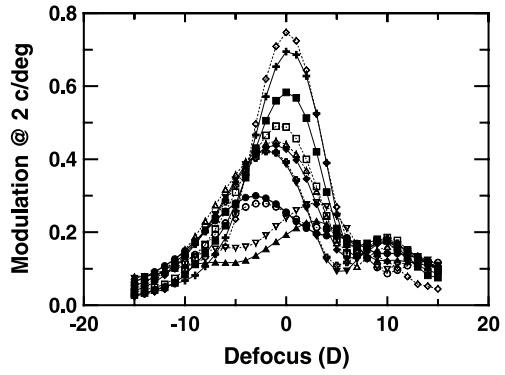

Fig. 5. Through-focus modulation transfer at 2 c/deg, estimated from radial profile MTFs. Each symbol corresponds to a different mouse eye. A positive defocus sign is indicative of positive defocus at the retinal plane (and therefore required myopic correction) and vice versa for negative defocus.

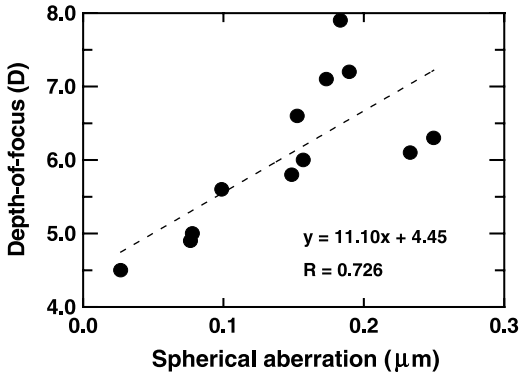

Fig. 6. Fourth order spherical aberration from Zernike expansion vs. depth-of-focus from through-focus modulation transfer at 2 c/deg using the Rayleigh criterion. Data are from 1.5-mm pupil diameter.

was used as another metric to obtain the depth-of-focus, and values ranging from 1.7 to 11 D were found using this metric. We found that depth-of-focus was highly correlated with the amount of individual fourth order spherical aberration present in each eye ($r = 0.726$, $p < 0.0001$), as shown in Fig. 6.

4. Discussion

4.1. The effect of anesthesia

While the measurement of the optical quality of the mouse eye under normal viewing conditions is important to get insights on the limits of spatial resolution, and to assess the prospects of the mouse as a myopia animal model, several applications will very likely require the use of anesthesia to immobilize the animal, for example in vivo retinal imaging. Also, previous measurements of the double-pass MTF in the rodent eye (Artal et al., 1998) were performed under total anesthesia (Equistesin). We compared measurements with and without anesthesia on the same eye (right eye of mouse # 2) to assess possible effects of the drug on optical quality. Measurements were attempted on other animals, but rapid opacification of the crystalline lens during anesthesia prevented completion of these measurements. We found larger HS spots in the anesthetized eye than in previous measurements under awake conditions on the same eye. We found higher amounts of aberrations in the anesthetized eye (RMS for third and higher order was 0.42 vs 0.32 μm in the awake eye; spherical aberration was 0.14 vs 0.09 μm; and RMS for third order was 0.32 vs 0.15 μm). We also found a lower hyperopic spherical equivalent in the anesthetized eye (+3.28 vs +10.12 D).

While these results are only for one eye, they may be indicative of larger optical degradation in anesthetized mouse eyes, and perhaps a possible cause of the differences in retinoscopic refractions from different authors (Beuerman et al., 2003; Schmucker & Schaeffel, 2004a; Tejedor & de la Villa, 2003). As previously reported (Calderone, Grimes, & Shalev, 1986), other additional complications further deteriorating optical quality under anesthesia may include corneal dryness and transient cataracts. While those are not accounted for by aberrometric MTFs they may contribute to decrease contrast of retinal images.

4.2. Comparisons with other studies: Refraction, MTF, and depth-of-focus

We found hyperopic defocus in the four-week old mouse eye of +9.7 ± 1.0 D (with the best-optical quality criterion) using Hartmann–Shack aberrometry at 680 nm, only slightly higher than that reported by Schmucker and Schaeffel (2004b) for mice of the same age (+7.0 ± 2.5 D) using infrared photoretinoscopy at 880 nm. These results are in contrast to previous studies using streak retinoscopy, reporting larger amounts of hyperopic defocus with eyelid suture [up to +13.5 D by (Tejedor & de la Villa, 2003)]. A control experiment performed by Schmucker and Schaeffel (2004b) demonstrates that chromatic aberration is not the cause for the discrepancy. The fact that the retinal reflection may occur in a retinal layer different from the photoreceptor layer, which is effectively aggravated in eyes with short focal lengths [the so-called ''small eye artifact''; (Glickstein & Millidot, 1970)], and reported differences with refractive errors obtained using visually evoked potentials (less hyperoropic), leaves the question open of whether the mouse eye is truly hyperopic. Additionally, Schmucker and Schaeffel (2004b) observed ring-shaped intensity distributions of the retinoscopic pupillary images, what led them to suggest that the crystalline lenses might be multifocal, similar to what has been described for fish eyes (Kroger, Campbell, Fernald, & Wagner, 1999). The spatial sampling resolution of our lenslets (400 μm) is too coarse to draw any conclusions regarding multifocality in the mouse eye.

We have computed MTFs from the measured wave aberrations in the mouse eye, for best focus (i.e., simulating correction of the measured hyperopia) and different amounts of defocus. The average MTF at best focus can

be compared with, to our knowledge, the only MTF previously reported, which corresponds to one single mouse eye, using a double-pass technique. While we found generally low MTFs, these are not as severely degraded as the MTF reported by Artal et al. (1998). While that study shows modulations lower than 0.1 for 1 c/deg for 1-mm, we found modulations close to 0.6 for that spatial frequency (see Fig. 4), for 1.5 mm pupils. There are several possible reasons for the discrepancy: (1) the previous study performed measurements under anesthesia, which appears to decrease image quality, and presumably increase corneal and intraocular scattering, which affects double-pass aerial images; (2) double-pass MTFs are likely affected by the presence of retinal scattering, producing halos in the aerial image resulting in a lower MTF; (3) the previous study only reports limited data on a single mouse, even though three animals were used as subjects, and the authors did not mention whether this was due to problems in data processing in the other two animals, or due to other reasons.

We have also obtained estimates of optical depth-of-focus, which can be compared with previous predictions and measurements from the literature. As shown by Fig. 5, the actual depth-of-focus will very much depend on the definition used. We found large depth-of-focus particularly in eyes with larger amounts of spherical aberration. However, our data of optical depth-of-focus are lower than previous predictions and reports using the double-pass method.

4.3. Implications of the results

Our results confirm previous speculations that higher order aberrations are major sources of optical quality degradation in the wild type mouse eye. Significant amounts of spherical aberrations are consistent with highly curved spherical surfaces, although a complete predictive model should incorporate aspheric surfaces and gradient index distributions in the crystalline lens. The presence of large amounts of third order aberrations and astigmatism may be due to eccentric fixations with respect to the optical axis. Interestingly, the high repeatability of the measured coma terms and relatively low intersubject variability seems to indicate that mouse use a certain fixation axis or did not make too large eye movements during the measurement, despite their afoveated retinas.

Even if we found severely degraded optics compared to the diffraction-limit, our MTF estimates for best-correction in the mouse are higher than previously reported using double-pass in one anesthetized mouse, and even rats. Even with defocus, the modulation at 1 c/deg is 0.2, which indicates that the optics do not impose the limits to spatial vision in the mouse eye. Behavioral and electrophysiological experiments report visual acuities of 0.5–0.6 c/deg (Gianfranceschi et al., 1999; Porciatti et al., 1999). The fact that anesthetized animals show larger amounts of aberrations than awake animals complicates further their correction for in vivo imaging. Provided that the second order aberrations are corrected by other means, current adaptive optics technology generally provides sufficient power to compensate the RMS measured in the anesthetized animal (0.5 μm). It seems more challenging to generate centroiding algorithms that process the severely degraded Hartmann–Shack in real time (our algorithms are accurate but not time-efficient), and to handle the presence of cataracts and corneal dryness.

The use of the mouse as an animal model for myopia has been challenging. Degrading the optical quality by diffusers (Schaeffel et al., 2004) or minus-lens power wear (Beuerman et al., 2003) has been shown to change the refractive state in the myopic direction but not all studies show the expected axial elongation. In fact, in one of the studies (Tejedor & de la Villa, 2003), the refractive and axial length change did not match at all. Our results show that moderate amounts of imposed spherical defocus (see Fig. 5) will not alter optical quality significantly, and therefore it is not surprising that mice do not respond to a lens treatment as consistently as other models. However, the measured optical depth-of-focus is lower than that estimated from behavioral measurements (Schmucker & Schaeffel, 2006), suggesting that tolerance to defocus may be ultimately limited by neural sampling. Our results show (see Fig. 4) that natural aberrations in the eye cause severe decrease in the contrast and spatial resolution of retinal images, even in the absence of defocus. In fact, if the hyperopic defocus measured using reflectometric techniques was caused by the small eye artefact the eye could be actually be nearly emmetropic, and the retinal image primarily blurred by the aberrations. This is very different to what we found in the chick model (García de la Cera et al., 2006), where the optics were almost diffraction-limited both in normal eyes and myopic eyes treated with diffusers (removing the defocus term). While in normal conditions chicks have high contrast retinal images, mice have much poorer retinal images (with defocus, and even without the hyperopic defocus, due to high order ocular aberrations alone). As opposed to what happens in chicks, the high tolerance to defocus and to further degradation by diffusers may make eye growth more challenging to respond to changes in visual experience, apart from other potential complicating factors such as the slow ocular growth (Schmucker & Schaeffel, 2004b).

Acknowledgments

This study was supported by Grant Nos. BFM-2002-02638 and FIS2005-04382 (Ministerio de Educación y Ciencia, España) to Susana Marcos, Acción-Integrada España-Alemania No. HA-2003-02638 (Ministerio de Educación y Ciencia, España) to Susana Marcos, and No. D/03/40332 (DAAD, Deutscher Akademischer Austauschdienst) to Frank Schaeffel. Elena García de la Cera acknowledges support of Beca Unidades Asociadas-CSIC. The authors also acknowledge the Unidad Asociada IOBA/Universidad de Valladolid—Instituto de Optica/

CSIC, as well as Jesús Merayo-Lloves and Christine Schmucker for assistance and helpful discussions.

References

Artal, P., Herreros de Tejada, P., Muñoz-Tedo, C., & Green, D. (1998). Retinal image quality in the rodent eye. *Visual Neuroscience, 15*, 597–605.

Barbero, S., Marcos, S., & Jimenez-Alfaro, I. (2003). Optical aberrations of intraocular lenses measured in vivo and in vitro. *Journal of the Optical Society of America A, 20*, 1841–1851.

Beuerman, R. W., Barathi, A., Weon, S. R., & Tan, D. (2003). Two models of experimental myopia in the mouse. *Investigative Ophthalmology & Visual Science, 44*(5), E-Abstract 4338.

Burns, S. A., Marcos, S., Elsnser, A. E., & Bará, S. (2002). Contrast improvement for confocal retinal imaging using phase correcting plates. *Optics Letters, 27*, 400–402.

Burns, S. A., Zhou, Y., Lin, C. P., Bifano, T. G., Veilleux, I., & Webb, R. H. (2004). Retinal imaging and wavefront sensing in mice. *Investigative Ophthalmology & Visual Science*, 45, E-Abstract 2787.

Calderone, L., Grimes, P., & Shalev, M. (1986). Acute reversible cataract induced by xylazine and by ketamine-xylazine anesthesia in rats and mice. *Experimental Eye Research, 42*(4), 331–337.

Chang, B., Hawes, N., Hurd, R., Davisson, M., Nusinowitz, S., & Heckenlively, J. (2002). Retinal degeneration mutants in the mouse. *Vision Research, 42*, 517–525.

García de la Cera, E., Rodriguez, G., & Marcos, S. (2006). Longitudinal changes of optical aberrations in normal and form-deprived myopic chick eyes. *Vision Research, 46*(4), 579–589.

Gianfranceschi, L., Fiorentini, A., & Maffei, L. (1999). Behavioural visual acuity of wild type and bcl2 transgenic mouse. *Vision Research, 39*(3), 569–574.

Glickstein, M., & Millidot, M. (1970). Retinoscopy and eye size. *Science, 168*, 605–606.

Green, D., Powers, M., & Banks, M. (1980). Depth of focus, eye size and visual acuity. *Vision Research, 20*, 827–835.

Guirao, A., & Williams, D. (2003). A method to predict refractive errors from wave aberration data. *Optometry and Visual Science, 80*, 36–42.

Hegde, K., Henein, M., & Varma, S. (2003). Establishment of the mouse as a model animal for the study of diabetic cataracts. *Ophthalmic Research*, 12–18.

Hughes, A. (1979). Schematic eye for the rat. *Vision Research, 19*(5), 569–588.

Hughes, & Wassle. (1979). An estimate of image quality in the rat eye. *Investigative Ophthalmology and Visual Science, 18*, 878–881.

Huxlin, K. R., Yoon, G., Nagy, L., Porter, J., & Williams, D. (2004). Monochromatic ocular wavefront aberrations in the awake-behaving cat. *Vision Research, 44*(18), 2159–2169.

Irving, E. L., Kisilak, M. L., Clements, K. M., & Campbell, M. C. W. (2005). Refractive error and optical image quality in three strains of albino rats. *Investigative Ophthalmology & Visual Science*, 46, E-Abstract 4334.

Kern, T., & Engerman, R. (1996). A mouse model of diabetic retinopathy. *Archives of Ophthalmology, 114*, 986–990.

Kroger, R., Campbell, M., Fernald, R., & Wagner, H. (1999). Multifocal lenses compensate for chromatic defocus in vertebrate eyes. *Journal of Comparative Physiology [A], 184*, 361–369.

Liang, J., & Williams, D. R. (1997). Aberrations and retinal image quality of the normal human eye. *Journal of the Optical Society of America A, 14*, 2873–2883.

Lin, C. P., Alt, C., Pierce, M., Wang, N., DeBoer, J., Burns, S. A., et al. (2004). Mouse eye parameters by optical coherence tomography (OCT). *Investigative Ophthalmology & Visual Science*, 45, E-Abstract 2786.

Lindsey, J., & Weinreb, R. (2005). Elevated intraocular pressure and transgenic applications in the mouse. *Journal of Glaucoma, 14*, 318–320.

Llorente, L., Diaz-Santana, L., Lara-Saucedo, D., & Marcos, S. (2003). Aberrations of the human eye in visible and near infrared illumination. *Optometry and Vision Science, 80*, 26–35.

Marcos, S., Barbero, S., & Jimenez-Alfaro, I. (2005). Optical quality and depth-of-field of eyes implanted with spherical and aspheric intraocular lenses. *Journal of Refractive Surgery, 21*(3), 223–235.

Marcos, S., Díaz-Santana, L., Llorente, L., & Dainty, C. (2002). Ocular aberrations with ray tracing and Shack-Hartmann wavefront sensors: Does polarization play a role? *Journal of the Optical Society of America A, 19*, 1063–1072.

Marcos, S., Moreno, E., & Navarro, R. (1999). The depth-of-field of the human eye from objective and subjective measurements. *Vision Research, 39*, 2039–2049.

Moreno-Barriuso, E., Marcos, S., Navarro, R., & Burns, S. A. (2001). Comparing laser ray tracing, spatially resolved refractometer and Hartmann–Shack sensor to measure the ocular wavefront aberration. *Optometry and Vision Science, 78*, 152–156.

Mutti, D. O., VerHoeve, J. N., Zadnik, K., & Murphy, C. J. (1997). The artifact of retinoscopy revisited: Comparison of refractive error measured by retinoscopy and visual evoked potential in the rat. *Optometry and Vision Science, 74*(7), 483–488.

Porciatti, V., Pizzorusso, T., & Maffei, L. (1999). The visual physiology of the wild type mouse determined with pattern VEPs. *Vision Research, 39*(18), 3071–3081.

Prusky, G. T., Alam, N. M., Beekman, S., & Douglas, R. M. (2004). Rapid quantification of adult and developing mouse spatial vision using a virtual optomotor system. *Investigative Ophthalmology & Visual Science, 45*(12), 4611–4616. doi:10.1167/iovs.04-0541.

Remtulla, S., & Hallett, P. E. (1985). A schematic eye for the mouse, and comparisons with the rat. *Vision Research, 25*(1), 21–31.

Ritter, M., Aguilar, E., Banin, E., Scheppke, L., Uusitalo-Jarvinen, H., & Friedlander, M. (2005). Three-dimensional in vivo imaging of the mouse intraocular vasculature during development and disease. *Investigative Ophthalmology & Visual Science, 46*, 3021–3026.

Roorda, A., & Willians, D. (2001). Retinal imaging using adaptive optics. In S. McRae, R. Krueger, & R. Applegate (Eds.), *Customized corneal ablation: The quest for super vision* (pp. 42–48). Stack publising.

Schaeffel, F., Burkhardt, E., Howland, H. C., & Williams, R. W. (2004). Measurement of refractive state and deprivation myopia in two strains of mice. *Optometry and Vision Science, 81*(2), 99–110.

Schmucker, C., & Schaeffel, F. (2004a). In vivo biometry in the mouse eye with low coherence interferometry. *Vision Research, 44*(21), 2445–2456.

Schmucker, C., & Schaeffel, F. (2004b). A paraxial schematic eye model for the growing C57BL/6 mouse. *Vision Research, 44*(16), 1857–1867.

Schmucker, C., & Schaeffel, F. (2006). Contrast sensitivity of wild type mice wearing diffusers or spectacle lenses, and the effect of atropine. *Vision Research, 46*(5), 678–687.

Seeliger, M. W., Beck, S. C., Pereyra-Munoz, N., Dangel, S., Tsai, J.-Y., Luhmann, U. F. O., et al. (2005). In vivo confocal imaging of the retina in animal models using scanning laser ophthalmoscopy. *Vision Research, 45*(28), 3512–3519.

Tejedor, J., & de la Villa, P. (2003). Refractive changes induced by form deprivation the mouse eye. *Investigative Ophthalmology & Visual Science, 44*(1), 32–36.

Thibos, L. N., Applegate, R. A., Schwiegerling, J. T., Webb, R. H., & Members, V. S. T. (2000). Standards for reporting the optical aberrations of eyes. *Vision Science and its Applications, OSA Trends in Optics & Photonics, 35*, 110–130.

Vilupuru, A. S., Roorda, A., & Glasser, A. (2004). Spatially variant changes in lens power during ocular accommodation in a rhesus monkey eye. *Journal of Vision, 4*(4), 299–309.